

MIND: Multi-rationale INtegrated Discriminative Reasoning Framework for Multi-modal Large Models

Chuang Yu^{1,2,3,6}, Jinmiao Zhao^{1,2,3}, Mingxuan Zhao⁴, Yunpeng Liu^{2†}, Xiuju Shu⁵, Yuanhao Feng⁵, Bo Wang⁵, Xiangyu Yue^{6†}

¹Key Laboratory of Opto-Electronic Information Processing, Chinese Academy of Sciences

²Shenyang Institute of Automation, Chinese Academy of Sciences ³University of Chinese Academy of Sciences

⁴HKUST(GZ) ⁵Tencent ⁶MMLab, The Chinese University of Hong Kong

<https://github.com/YuChuang1205/MIND>

Abstract

Recently, multimodal large language models (MLLMs) have been widely applied to reasoning tasks. However, they suffer from limited multi-rationale semantic modeling, insufficient logical robustness, and are susceptible to misleading interpretations in complex scenarios. Therefore, we propose a Multi-rationale INtegrated Discriminative (MIND) reasoning framework, which is designed to endow MLLMs with human-like cognitive abilities of “Understand → Rethink → Correct”, and achieves a paradigm evolution from passive imitation-based reasoning to active discriminative reasoning. Specifically, we introduce a Rationale Augmentation and Discrimination (RAD) paradigm, which automatically and efficiently expands existing datasets by generating diverse rationales, providing a unified and extensible data foundation. Meanwhile, we design a Progressive Two-stage Correction Learning (P2CL) strategy. The first phase enhances multi-rationale positive learning, while the second phase enables active logic discrimination and correction. In addition, to mitigate representation entanglement in the multi-rationale semantic space, we propose a Multi-rationale Contrastive Alignment (MCA) optimization strategy, which achieves semantic aggregation of correct reasoning and boundary separation of incorrect reasoning. Extensive experiments demonstrate that the proposed MIND reasoning framework achieves state-of-the-art (SOTA) performance on multiple public datasets covering scientific, commonsense, and mathematical scenarios. It provides a new perspective for advancing MLLMs towards higher levels of cognitive intelligence.

1. Introduction

With the rapid advancement of multimodal large language models (MLLMs) across tasks such as visual question answering (VQA) [4, 6, 53, 67], visual reasoning [9, 54, 66], and cross-modal understanding [15, 16, 61], reasoning ability has emerged as a key indicator of a model’s intelligence. To enhance this, recent research has proposed Multimodal

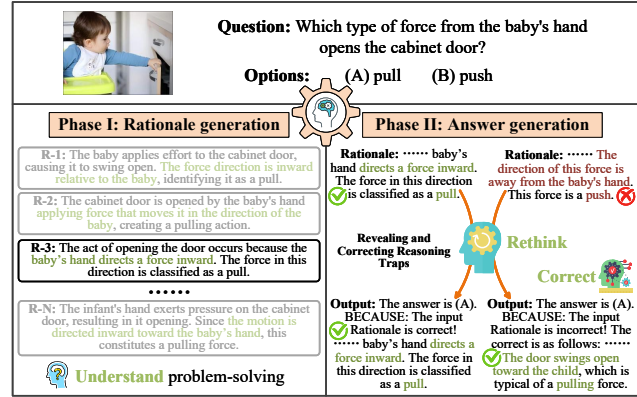


Figure 1. Illustration of MIND’s “Understand → Rethink → Correct” paradigm. It consists of two phases: Rationale (reasoning chain) generation and Answer generation. In **Phase I**, the model focuses on understanding the essential elements of problem-solving. In **Phase II**, the model rethinks the generated rationales and corrects erroneous reasoning logic.

Chain-of-Thought (MCoT) [74], which incorporates intermediate reasoning steps. This allows models to generate reasoning chains in a step-by-step manner, thereby improving logical transparency [58]. However, existing MCoT methods [13, 49, 55, 74, 76] still predominantly rely on single-rationale supervision during training. This paradigm tends to drive models to learn only the surface-level mapping toward a standard answer, failing to capture the diversity and complexity inherent in human reasoning. Consequently, when confronted with ambiguous, incorrect, or misleading explanations, these models often exhibit rigid reasoning patterns, weak logical robustness, and limited reasoning discrimination or self-correction capabilities. In contrast, human reasoning is not a static, linear process but rather a dynamic cycle involving diverse rationales, reflective falsification, and self-correction [69].

Current MLLMs generally lack the ability to model and discriminate among diverse rationale relations, making them vulnerable to misleading or adversarial information in complex scenarios. We believe that relying solely on single-rationale supervision fails to capture the diversity

and self-corrective nature of human reasoning. As shown in Fig. 1, MLLMs need learn both the semantic consistency of correct reasoning and the discriminative boundaries of incorrect reasoning within a multi-rationale space, and further develop self-correcting capabilities, thereby facilitating a paradigm evolution from passive imitation-based reasoning to active discriminative reasoning. Therefore, endowing MLLMs with the capability to understand multiple rationales, identify logical inconsistencies, and perform self-correction is crucial for advancing intelligent reasoning from imitation to true cognition intelligence.

Based on the above motivation, we propose the first Multi-rationale INtegrated Discriminative (MIND) reasoning framework for MLLMs. Unlike traditional single-rationale supervision, MIND incorporates diverse positive rationales to model the diversity of human reasoning, while simultaneously leveraging challenging negative rationales to reveal potential reasoning pitfalls. Specifically, we propose a Rationale Augmentation and Discrimination (RAD) paradigm that automatically and efficiently generates diverse rationales. Unlike conventional datasets that provide only a single rationale, RAD adopts a positive/negative co-generation mechanism to explicitly model diverse reasoning and potential reasoning traps, providing a unified and extensible data foundation. Meanwhile, inspired by the human cognitive process of “Understand → Rethink → Correct”, we design a Progressive Two-stage Correction Learning (P2CL) strategy to drive the evolution from passive imitation-based reasoning to active discriminative reasoning. In Phase I, diverse positive rationales are used to enhance semantic understanding and multi-rationale logical modeling, while Phase II leverages both positive and negative rationales to guide the model in identifying and correcting erroneous reasoning, forming a self-reflective and logic-repairing reasoning mechanism. Additionally, to further improve the model’s discriminative ability within the multi-rationale semantic space, we propose a Multi-rationale Contrastive Alignment (MCA) optimization strategy. By aggregating hard positive rationales and separating hard negative rationales in the embedding space, MCA adaptively expands semantic boundaries, significantly enhancing the model’s logical consistency and discrimination sensitivity. The contributions can be summarized as follows:

- We propose the first MIND reasoning framework for MLLMs. By introducing diverse positive rationales to model the diversity of human reasoning and incorporating challenging negative rationales to reveal and correct potential reasoning pitfalls, MIND drives a paradigm evolution from passive imitation-based reasoning to active discriminative reasoning.
- We develop a RAD paradigm that automatically and efficiently generates diverse positive rationales and semantically inverted challenging negative rationales, providing

a unified and extensible data foundation.

- Inspired by the human cognitive mechanism, we design a P2CL strategy. The first phase enhances multi-rationale positive learning, while the second phase enables active logic discrimination and correction.
- To further enhance discrimination, we construct a MCA optimization strategy that achieves effective positive rationale aggregation and semantic conflict separation.

2. Related Work

Prompt-based MCoT Reasoning aims to enhance multimodal reasoning ability by explicitly inducing models to generate step-by-step reasoning through carefully designed prompts. Typical methods adopt prompts such as “Let’s think step by step!” to encourage sequential reasoning, while employing explicit task planning or fixed reasoning templates to constrain logical paths [5, 37, 40, 48, 57, 63, 72, 75]. To further strengthen visual-semantic understanding, some studies incorporate external tools [11, 30, 50, 64] or transform visual features into textual form [14, 39, 62], allowing language models to better fuse cross-modal information. Prompt-based methods require no additional training and are highly flexible, making them well-suited for resource-constrained tasks. However, their performance is highly dependent on prompt quality and they lack error discrimination and correction mechanisms, making them prone to logical drift or hallucination [58].

Learning-based MCoT Reasoning explicitly models the reasoning generation process during training, enabling models to internalize reasoning abilities through supervised learning. As an early milestone, Multimodal-CoT [74] established a two-stage learning framework that paved the way for later studies [13, 49, 55, 76]. Subsequently, MC-CoT [49] enhances the logical robustness of smaller models by introducing multimodal consistency constraints and majority-voting mechanisms. T-SciQ [55] leverages high-quality rationales generated by powerful language models for cross-modal reasoning transfer. To further alleviate hallucination, several works explore combining diffusion models or retrieval-based models as auxiliary tools [9, 23, 24, 28, 39, 62, 77]. For example, VoT [62] enables text-only models to imagine visual reasoning paths. Overall, learning-based methods demonstrate stronger logical consistency and semantic stability than prompt-based methods. However, existing methods rely heavily on single-rationale supervision and lack mechanisms for identifying and correcting erroneous reasoning. To address these limitations, this paper aims to endow MLLMs with human-like cognitive abilities of “Understand → Rethink → Correct”, achieving a paradigm evolution from passive imitation-based reasoning to active discriminative reasoning.

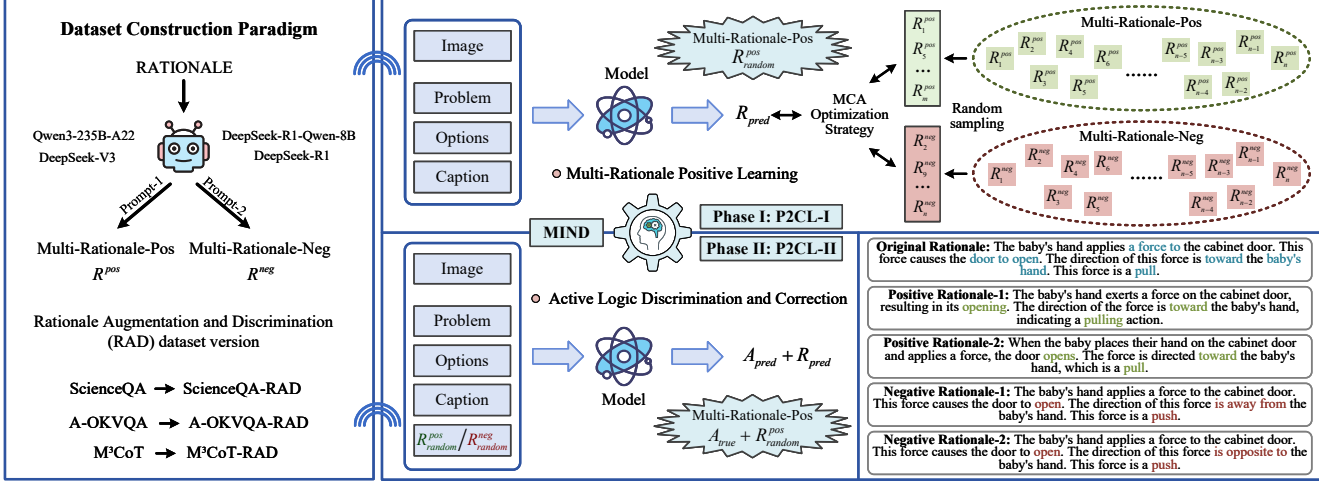


Figure 2. Overview of the MIND reasoning framework. The blue circle denotes the format of the supervision signal.

3. Methods

3.1. Overview

Inspired by the human cognitive processes, we propose the MIND reasoning framework. As shown in Fig. 2, MIND consists of two key components: the RAD dataset construction paradigm and the MIND learning architecture. For the data construction, the RAD paradigm provides MIND with multi-rationale training samples. By well-designed positive and negative prompts, existing large models are guided to generate diverse positive rationales and challenging negative rationales under controlled conditions. For the model learning, the MIND aims to enhance human-like cognitive ability. Unlike conventional methods that rely on single-rationale supervision, MIND incorporates diverse positive and negative rationales during training and employs a P2CL strategy to achieve alignment with the human cognitive pattern of “Understand → Rethink → Correct”. Specifically, Phase I (P2CL-I) focuses on multi-rationale positive learning. This phase encourages the MLLMs to grasp the essence of problem-solving (understanding) rather than direct mapping relationships (rote memorization). Phase II (P2CL-II) emphasizes active logic discrimination and correction, using both positive and negative rationales to identify and correct reasoning errors. In addition, the MIND incorporates a MCA optimization strategy, which enforces semantic aggregation across consistent rationales and separation of conflicting semantics. In summary, the proposed MIND, through the synergistic interaction of RAD, P2CL and MCA, achieves a transition from shallow imitative reasoning to deep cognitive reasoning.

3.2. RAD Paradigm

To generate diverse rationales, we propose a RAD dataset construction paradigm, which systematically generates di-

verse positive rationales and semantically inverted negative rationales to model the diversity and discriminative nature of human reasoning. Unlike conventional VQA datasets [4, 34, 46] that provide a single standard rationale, RAD offers a unified and extensible data foundation.

From Fig. 3, for each sample $S = \{I, Q, O, C, A, R_{gt}\}$ consisting of an image I , question Q , options O , image caption C , answer A , and the original rationale R_{gt} , we design a structured prompt template to guide existing large models to automatically and efficiently generate diverse rationales. To mitigate the high computational and time costs of generating rationales one by one, RAD adopts a batch-wise generation mechanism in its prompt design, allowing multiple rationales to be generated in a single interaction, which significantly improves data construction efficiency. In addition, to ensure that the generated rationales meet semantic requirements, we incorporate task-related information, such as the question, options, and answer, into the input to help large models better understand the reasoning context and semantic constraints, thereby avoiding the generation of rationales that do not meet the requirements. Specifically, we design two types of prompts: **Positive Prompts** and **Negative Prompts**. The detailed designs are as follows:

Positive Prompts: “{Task-related information}”\n You are an intelligent agent with both perception and reasoning abilities. Based on the given context, please make random content adjustments to “{Solution}” within a range of 10% to 50% while ensuring that the semantics remain unchanged. Please output {Repeat_number} different solutions. Each output format is “Adjusted Solution:”. Use “\n\n~~~\n\n” to separate them. The output must be in the required format.

Negative Prompts: “{Task-related information}”\n You are an intelligent agent with both perception and reasoning abilities. “{Solution}” is the explanation for

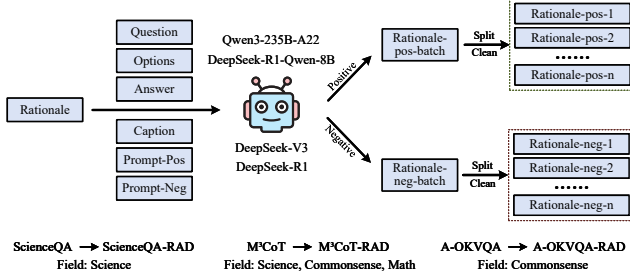


Figure 3. Overview of the RAD paradigm.

the above problem. Based on the given context, please make minor edits to “*{Solution}*” to reverse its meaning and ensure the correct answer cannot be logically derived, while keeping most of the original words and structure intact. Please output *{Repeat_number}* different solutions. Each output format is “Negative Solution:”. Use “\n\n~~~\n\n” to separate them. The output must be in the required format.

Under the guidance of the above prompts, the large model generates multiple candidate rationales for each sample. We then perform rationale splitting and cleaning to ensure that the generated content adheres to both format and semantic standards. Specifically, the model output is first split using the predefined delimiter “\n\n~~~\n\n”, separating the batch-generated rationales into individual samples. Next, each rationale undergoes filtering and cleaning to ensure textual conciseness and consistency. All valid positive and negative rationales are stored separately in *Multi-Rationale-Pos* and *Multi-Rationale-Neg* pools, forming the final multi-rationale augmented sample:

$$S_{RAD} = \{I, Q, O, C, A, R_{gt}, \{R_i^+\}, \{R_j^-\}\}, \quad (1)$$

where $\{R_i^+\}$ and $\{R_j^-\}$ denotes the set of positive rationales and negative rationales. This collaborative design of positive and negative prompts provides high-quality and well-structured training sample for subsequent MIND learning.

3.3. P2CL Strategy

Inspired by the human cognitive patterns of “Understand → Rethink → Correct”, we design a P2CL strategy. This strategy divides the training process into two complementary phases: multi-rationale positive learning (P2CL-I) and active logic discrimination and correction (P2CL-II).

In P2CL-I, the model uses random sampling in the *Multi-Rationale-Pos* pool as supervision, aiming to learn the shared causal and logical chains expressed in different linguistic forms, thereby avoiding overfitting to a single standard rationale. Given a multimodal sample $S_{RAD} = \{I, Q, O, C, R_{gt}, \{R_i^+\}_{i=1}^M\}$, the model jointly encodes visual and textual via the multimodal encoder and a language decoder to generate the rationale \hat{R} . We employ a maximum

likelihood generation objective to encourage the model to capture consistent logic across diverse rationales:

$$\mathcal{L}_{\text{pos}} = -\mathbb{E}_{R^+} \sum_t \log p(\hat{R}_t^+ | I, Q, O, C). \quad (2)$$

To further enhance the semantic boundaries discrimination and embedding consistency, P2CL-I is jointly optimized with the MCA optimization strategy (please see Sec. 3.4), whose loss term is denoted as \mathcal{L}_{mca} . Thus, the total optimization objective of P2CL-I is as follow:

$$\mathcal{L}_{P-I} = \mathcal{L}_{\text{pos}} + \alpha \cdot \mathcal{L}_{\text{mca}} \quad (3)$$

In P2CL-II, the model uses positive-negative rationale pairs $R_{\text{cond}} \in \{R_i^+, R_j^-\}$ as semantic cues, and explicitly models error identification and logical correction through a unified joint generation objective for both answers and rationales. Given a multimodal sample input $Q' = \{I, Q, O, C, R_{\text{cond}}\}$, the model takes either a positive or negative rationale as input and generates a concatenated output sequence of the answer and rationale $[\hat{A}, \hat{R}^+]$:

$$\mathcal{L}_{P-II} = -\mathbb{E}_{R_{\text{cond}}} \sum_t \log p([\hat{A}, \hat{R}_t^+] = [A, R_t^+] | Q'), \quad (4)$$

where A and R_t^+ denote the correct answer and the target rationale, respectively. When the input rationale is positive, the model is constrained to maintain expression stability. When the input rationale is negative, the model is required to identify logical deviations in the rationale and correct them. P2CL-II enhances the model’s discriminative reasoning and logical correction capabilities.

After the two-stage training, the model learns semantic consistency, discriminative boundaries, and self-corrective capability. The P2CL strategy drives a paradigm evolution from passive imitation-based reasoning to active discriminative reasoning, empowering the model with human-like cognitive capabilities.

3.4. MCA Optimization Strategy

Although the P2CL strategy progressively establishes semantic consistency and discriminative reasoning ability, representation instability may still occur within the multi-rationale semantic space. To address this issue, we further propose a MCA optimization strategy, which explicitly enforces the semantic aggregation of correct rationales and separation of incorrect rationales in the embedding space through a hard-rationale mining mechanism and contrastive semantic constraints.

First, the multimodal encoder and language decoder jointly model the multimodal inputs to obtain the predicted embedding, which is then projected into a unified semantic contrastive space via a linear mapping layer $g_\phi(\cdot)$. For each sample, the sets of positive and negative rationales are

denoted as $\{R_i^+\}$ and $\{R_j^-\}$, respectively. After encoding, their embeddings can be represented as:

$$h^{+/-} = g_\phi(f_\theta(I, Q, O, C, R^{+/-})). \quad (5)$$

Second, we randomly sample N rationales from both positive and negative sets and compute their cosine similarities with predicted embedding in each iteration:

$$s_i^+ = \text{sim}(h_{\text{pred}}, h_i^+), \quad s_j^- = \text{sim}(h_{\text{pred}}, h_j^-). \quad (6)$$

Third, to focus effective parameter updates guided by the most discriminative rationales, the MCA strategy performs dual hard rationale mining for both positive and negative sets. For positive rationales $\{s_i^+\}$, the Bottom-k (with the lowest similarity) is selected. For negative rationales $\{s_j^-\}$, the Top-k (with the highest similarity) is selected:

$$S_{\text{hard}}^+ = \text{Bottom-}k(\{s_i^+\}), \quad S_{\text{hard}}^- = \text{Top-}k(\{s_j^-\}). \quad (7)$$

Finally, to explicitly enlarge the distance between positive and negative rationales in the embedding space, we define a margin-based contrastive loss:

$$\mathcal{L}_{\text{con}} = \text{ReLU}(\bar{S}_{\text{hard}}^- + m - \bar{S}_{\text{hard}}^+), \quad (8)$$

where m is the margin. \bar{S}_{hard}^- and \bar{S}_{hard}^+ denote the mean cosine similarities of the negative Top-k and positive Bottom-k rationales, respectively. This loss encourages the model to pull closer the hard positive rationales and push away the hard negative rationales, thereby forming clear semantic boundaries in the embedding space.

Directly using contrast constraints may prematurely force the aggregation or separation of rationales before the semantic space has fully converged, potentially increasing the risk of semantic collapse and representation drift. Therefore, the MCA strategy is coupled with the P2CL-I to achieve synergistic optimization between generative supervision and contrastive alignment in our experiments. This mechanism suppresses semantic divergence in early training and reinforces logical consistency in later stages, ultimately enabling the model to form a stable.

4. Experiments

4.1. Datasets

We conduct systematic experiments on three VQA datasets covering different domains, namely, ScienceQA [34], A-OKVQA [46], and M³CoT [4]. ScienceQA focuses on science and contains 21,208 samples. A-OKVQA targets commonsense question answering and includes 24,903 samples. M³CoT integrates science, commonsense, and mathematics, comprising 11,328 samples. For all datasets, the data partitioning remains consistent with their original versions to ensure fair comparison. Meanwhile, based on the

proposed RAD paradigm, we build corresponding RAD-extended versions for each dataset, namely ScienceQA-RAD, A-OKVQA-RAD, and M³CoT-RAD. Compared with original, the rationales in these RAD versions are expanded by factors of 1000x, 1000x, and 500x, respectively.

4.2. Implementation Details

Following previous research settings, we adopt a T5-based encoder-decoder architecture [45] and explore two model scales: Base (223M) and Large (738M). The model is initialized with FLAN-Alpaca weights [7]. Visual features are extracted using a frozen BLIP2-flan-t5-xxl [26] encoder, while image captions are generated by Qwen2.5-VL-72B [3]. The learning rate and batch size are set to $8e^{-5}$ and 8. The hyperparameters m and α are set to 0.2 and 1. The maximum input sequence length is 512. Considering the varying complexity of different datasets, the number of training epochs is set to 200 for ScienceQA-RAD, and 400 for A-OKVQA-RAD and M³CoT. All experiments are conducted on eight 96GB NVIDIA H20 GPUs.

4.3. Comparison with SOTA Methods

We conduct systematic comparisons with a variety of excellent methods. Since MIND is developed upon Multimodal-CoT, we particularly highlight the performance comparison with it to show the performance improvements. More visualizations can be found in the Supplementary Materials.

1) Evaluation on the ScienceQA dataset. As shown in Tab. 1, the MIND_{base} model achieves an average accuracy of 92.29%, reaching the current SOTA performance. First, compared to early VQA and cross-modal understanding models (e.g., MCAN [71]), MIND_{base} achieves approximately 30% improvement. Second, compared to large language models such as GPT-3.5 [34], MIND_{base} outperforms these by 0.54% - 18.32%. Third, for larger MLLMs (such as LLaVA [31]), MIND_{base} achieves 1.37% - 7.10% improvement with only 223M parameters. Finally, compared with recent multimodal CoT-based methods, our MIND_{base} achieves superior performance with the same or fewer parameters. Compared to MC-CoT_{base} [49], DPMM-CoT_{base} [13], and Multimodal-T-SciQ_{base} [55], MIND_{base} improves performance by 1.65% (from 90.64% to 92.29%), 1.32% (from 90.97% to 92.29%), and 0.32% (from 91.97% to 92.29%), respectively. Notably, compared to Multimodal-CoT [74], MIND_{base} improves 6.98%.

2) Evaluation on the A-OKVQA dataset. Compared to ScienceQA, A-OKVQA has a stronger knowledge dependency and openness. From Tab. 2, MIND_{base} achieves an accuracy of 70.6%, reaching the current SOTA performance. First, compared to CoT-based Few-shot methods (such as IPVR [5]), MIND_{base} achieves an accuracy improvement of 11.9% - 25.5%. Second, compared to the visual-language fine-tuning methods, MIND_{base} out-

Table 1. Main results (%) on the ScienceQA dataset. Learning = Learning and training methods. Size = backbone model size. NAT = natural science, SOC = social science, LAN = language science, TXT = text context, IMG = image context, NO = no context, G1-6 = grades 1-6, G7-12 = grades 7-12. **Red** denotes the best result, and **blue** denotes the second best result.

Model	Learning	Size	NAT	SOC	LAN	TXT	IMG	NO	G1-6	G7-12	Avg
Random	-	-	40.28	46.13	29.25	47.45	40.08	33.66	39.35	40.67	39.83
Human	-	-	90.23	84.97	87.48	89.60	87.50	88.10	91.59	82.42	88.40
MCAN [71]	Fine-tune	95M	56.08	46.23	58.09	59.43	51.17	55.40	51.65	59.72	54.54
Top-Down [2]	Fine-tune	70M	59.50	54.33	61.82	62.90	54.88	59.79	57.27	62.16	59.02
BAN [20]	Fine-tune	112M	60.88	46.57	66.64	62.61	52.60	65.51	56.83	63.94	59.37
DFAF [10]	Fine-tune	74M	64.03	48.82	63.55	65.88	54.49	64.11	57.12	67.17	60.72
ViLT [21]	Fine-tune	113M	60.48	63.89	60.27	63.20	61.38	57.00	60.72	61.90	61.14
Patch-TRM [33]	Fine-tune	90M	65.19	46.79	65.55	66.96	55.28	64.95	58.04	67.50	61.42
VisualBERT [27]	Fine-tune	111M	59.33	69.18	61.18	62.71	58.54	62.96	59.92	61.87	
GPT-3.5 [34]	Few-shot	175B	74.64	69.74	76.00	74.44	67.28	77.42	76.80	68.89	73.97
GPT-3.5 w/ coT [59]	Few-shot	175B	75.44	70.87	78.09	74.68	67.43	79.93	78.23	69.68	75.17
ChatGPT w/ coT [1]	Few-shot	175B	78.82	70.98	83.18	77.37	67.92	86.13	80.72	74.03	78.31
GPT-4 w/ coT [1]	Few-shot	-	85.48	72.44	90.27	82.65	71.49	92.89	86.66	79.04	83.99
Chameleon (ChatGPT) [35]	Few-shot	-	81.62	70.64	84.00	79.77	70.80	86.62	81.86	76.53	79.93
Chameleon (GPT-4) [35]	Few-shot	-	89.83	74.13	89.82	88.27	77.64	92.13	88.03	83.72	86.54
Gemini+RMR [50, 52]	Few-shot	-	91.79	94.26	89.64	91.40	89.69	91.01	92.84	89.78	91.75
LLaMA-Adapter [73]	Fine-tune	6B	84.37	88.30	84.36	83.72	80.32	86.90	85.83	84.05	85.19
LLaVA [31]	Fine-tune	13B	90.36	95.95	88.00	89.49	88.00	90.66	90.93	90.90	90.92
LaVIN [36]	Fine-tune	7B	89.25	94.94	85.24	88.51	87.46	88.08	90.16	88.07	89.41
UnifiedQA _{base} [19]	Fine-tune	223M	68.16	69.18	74.91	63.78	61.38	77.84	72.98	65.00	70.12
UnifiedQA _{base} w/ coT [34]	Fine-tune	223M	71.00	76.04	78.91	66.42	66.53	81.81	77.06	68.82	74.11
DDCoT _{base} [76]	Fine-tune	223M	88.72	86.84	84.91	87.59	83.34	88.08	88.58	85.10	87.34
MC-CoT _{base} [49]	Fine-tune	223M	91.87	84.59	93.00	92.28	88.30	92.75	90.64	90.64	90.64
DPMM-CoT _{base} [13]	Fine-tune	306M	92.72	87.85	89.91	92.72	90.48	91.29	91.45	90.11	90.97
Multimodal-T-SciQ _{base} [55]	Fine-tune	223M	91.52	91.45	92.45	91.94	90.33	92.26	92.11	91.10	91.75
Multimodal-CoT _{base} [74]	Fine-tune	223M	84.06	92.35	82.18	82.75	82.75	84.74	85.79	84.44	85.31
MIND_{base} (Ours)	Fine-tune	223M	93.07	96.74	87.09	92.42	92.76	89.27	92.91	91.17	92.29
Improvement	-	-	9.01 \uparrow	4.39 \uparrow	4.91 \uparrow	9.67 \uparrow	10.01 \uparrow	4.53 \uparrow	7.12 \uparrow	6.73 \uparrow	6.98 \uparrow

Table 2. Results (%) on the Multiple-Choice task of A-OKVQA dataset. **Red** marks the best result, and **blue** the second best.

Model	Learning	Acc.	Model	Learning	Acc.
CoT [59]	Few-shot	48.1	Pythia [17]	Fine-tune	49.0
Pica [68]	Few-shot	46.1	ViLBERT [32]	Fine-tune	49.1
ClipCap [41]	Few-shot	56.9	LXMERT [51]	Fine-tune	51.4
IPVR (OPT-66B) [5]	Few-shot	48.6	KRISP [38]	Fine-tune	51.9
IPVR (GPT-3) [5]	Few-shot	58.7	GPV-2 [18]	Fine-tune	60.3
Multimodal-CoT _{base}	Fine-tune	50.6	MIND_{base}	Fine-tune	70.6

performs by 10.3% - 21.6%. Finally, compared with Multimodal-CoT_{base} [74], our MIND_{base} achieves a remarkable 20.0% improvement (from 50.6% to 70.6%).

3) **Evaluation on the M³CoT dataset.** From Tab. 3, MIND_{base} achieves an average accuracy of 57.38%, outperforming Multimodal-CoT_{base} and MC-CoT_{base} by 12.53% and 3.87%, respectively. Meanwhile, the extended MIND_{large} model surpasses Multimodal-CoT_{large} and MC-CoT_{large} by 12.83% and 3.87%, respectively. In addition, MIND has more prominent advantages compared to other types of models. First, for tool-enhanced models such as HuggingGPT [47], MIND achieves significantly better performance, demonstrating the efficiency of its intrinsic reasoning mechanism. Secondly, for zero-shot multimodal large models, their overall accuracy is only 23.17%

- 56.95%. Compared to the optimal GPT-4V, MIND_{large} (738M) achieves a 4.61% improvement at a smaller model size. Finally, for conventional fine-tuning models such as LLaMA-Adapter [73], MIND_{large} achieves 2.06% - 6.67% improvement with fewer parameters.

4.4. Ablation Experiment

To fully validate the proposed MIND reasoning framework, we perform detailed ablation experiments. More experiments can be found in the Supplementary Materials.

1) Break-Down Ablation. From Tab. 4, when only the MCA optimization strategy is applied, the model achieves a improvement of 0.07%, indicating that MCA facilitates semantic alignment and feature aggregation, though its standalone impact remains limited. Meanwhile, applying only the P2CL strategy yields a significant gain of 1.86%, demonstrating that multi-rationale positive learning and active logic discrimination and correction play a crucial role in enhancing reasoning. Furthermore, when both strategies are combined, the model performance further rises to 92.29%, achieving a “1 + 1 > 2” synergistic effect. These results verify the complementarity between P2CL and MCA, whose collaboration jointly optimizes semantic coherence.

2) Investigating the impact of the rationale quality and

Table 3. Main results (%) on the M³CoT dataset. ‘‘Random’’ and ‘‘Human’’ performance are the average accuracy by three attempts. **Red** denotes the best result, and **blue** denotes the second best result.

Model	Size	Science			Commonsense			Mathematics			Total
		Lang	Natural	Social	Physical	Social	Temporal	Algebra	Geometry	Theory	
Random	-	32.70	30.62	26.71	32.97	22.22	20.33	35.71	27.50	23.81	28.56
Human	-	97.83	92.62	94.31	96.28	92.41	88.71	87.23	88.75	85.71	91.61
<i>Tool-Usage Methods</i>											
HuggingGPT [47]	175B	17.57	20.93	10.33	8.70	14.75	9.76	11.35	22.50	9.52	14.60
VisualChatGPT [60]	>175B	30.09	36.28	7.78	43.48	29.92	33.33	21.99	21.25	28.57	25.92
IdealGPT [70]	-	31.73	31.63	26.23	56.52	50.00	26.83	20.57	30.00	38.10	32.19
Chameleon [35]	-	43.87	26.05	25.44	39.13	37.30	48.78	17.73	26.25	23.81	34.29
<i>Zero-shot Methods</i>											
Kosmos-2 [43]	2B	10.43	28.61	21.18	33.33	17.77	28.46	21.43	21.25	14.29	23.17
InstructBLIP [8]	13B	38.39	30.52	26.27	76.67	70.66	35.77	30.00	22.50	19.05	35.94
LLava-V1.5 [31]	13B	36.97	27.46	20.22	52.22	23.55	27.64	22.86	45.00	4.76	27.05
CogVLM [56]	17B	52.61	37.42	26.91	55.56	54.13	29.27	29.29	32.50	23.81	37.19
Gemini [52]	-	73.93	41.25	31.21	56.67	71.49	62.60	30.71	27.50	28.57	45.17
GPT4V [1]	-	80.09	54.66	43.95	87.78	67.77	82.11	42.14	43.75	42.86	56.95
<i>Finetuning Methods</i>											
LLaMA-Adaper [73]	7B	62.56	72.29	30.21	76.92	59.67	72.36	30.71	38.75	38.10	54.89
LLaVA-V1.5 [31]	13B	68.72	72.41	40.86	83.52	64.61	69.11	35.71	45.00	38.10	59.50
CogVLM [56]	17B	65.88	77.52	29.09	81.32	65.43	75.61	35.71	46.25	47.62	58.25
MC-CoT _{base} [49]	223M	53.55	63.98	43.56	61.54	69.55	29.27	42.86	33.75	28.57	53.51
MC-CoT _{large} [49]	738M	42.65	67.43	50.56	58.24	60.49	56.10	57.86	62.50	14.29	57.69
Multimodal-CoT _{base} [74]	223M	41.71	46.49	39.90	59.34	60.91	27.64	48.57	35.00	28.57	44.85
MIND_{base} (Our)	223M	72.04	63.09	43.31	82.22	65.29	44.72	49.29	61.25	33.33	57.38
Improvement	-	30.33 ↑	16.60 ↑	3.41 ↑	22.88 ↑	4.38 ↑	↑ 17.08	0.72 ↑	26.25 ↑	4.76 ↑	12.53 ↑
Multimodal-CoT _{large} [74]	738M	45.50	50.19	43.56	63.74	64.61	33.33	40.71	61.25	28.57	48.73
MIND_{large} (Our)	738M	79.62	66.41	48.57	81.11	69.42	51.22	50.71	61.25	47.62	61.56
Improvement	-	34.12 ↑	16.22 ↑	5.01 ↑	17.37 ↑	4.81 ↑	17.89 ↑	10.00 ↑	0.00 ↑	19.05 ↑	12.83 ↑

quantity. On the one hand, to evaluate the impact of the rationale quality, we conduct a comparative analysis among the DeepSeek series [12, 29], Qwen series [65]. From Tab. 5, with the improvement of the generation model’s capability, the performance consistently increases. Specifically, when using rationales generated by DeepSeek-R1-Qwen8B, the accuracy reaches 91.49%. Further employing the more powerful Qwen3-235B-22A for rationale generation boosts the accuracy to 91.61%, indicating that rationales produced by stronger models possess higher semantic completeness and logical consistency. In comparison, rationales generated by DeepSeek V3 yield limited improvement. Notably, Deepseek-R1 has only one-third the Rationales of the others. Ultimately, the ‘‘Final Mix’’ achieves the best performance, which verifies that the multi-source generation strategy can effectively leverages the complementary strengths of different models in semantic coverage and logical reasoning. On the other hand, we further evaluated MIND under different rationale scales. From Tab. 6, the model’s accuracy steadily improves as the number of rationales increases, though the gain gradually saturates. Specifically, compared to ‘‘Original (21K)’’, using more rationales resulted in a performance improvement of 1.13%-2.00%. In addition, when the number of rationales reaches $\times 1000$ (21M), the performance increase tends to level off, indicating that the model’s ability is close to saturation under ultra-large-scale rationales.

3) Investigation of Epochs, Caption Generation, and Visual Feature Extraction. From Fig. 4, model performance improves steadily with an increasing number of training epochs. The performance gain is pronounced when the number of epochs increases from 20 to 50, while the improvement gradually plateaus beyond 50 to 200 epochs. In this work, we adopt 200 epochs as the default setting for all experiments. Regarding image caption generation, we compare InstructBLIP [8] and Qwen2.5-VL [3]. As shown in Fig. 4, larger models with stronger semantic and visual alignment abilities (e.g., Qwen2.5-VL-72B) produce more complete and coherent captions, thereby improving rationale consistency and answer reliability. For visual feature extraction, the results are shown in Tab. 7. On the one hand, larger-scale visual encoders provide more solid visual grounding for reasoning. For instance, SAM-Huge [22] and DINOv2-Giant [42] preserve detailed structures while reinforcing global semantic coherence, thereby improving reasoning accuracy. On the other hand, multimodal models with language enhancement mechanisms (such as CLIP-L14-336 [44] and BLIP2-flan-t5-xxl [26]) establish a closer semantic mapping between vision and text, enabling the model to more accurately align the semantics of the image and text when generating rationales and answers. This demonstrates that higher-level semantic representation and stronger cross-modal alignment capabilities are key factors in improving reasoning performance.

Table 4. Break-Down ablation on the ScienceQA dataset.

Schemes	P2CL	MCA	Acc.	Improve.
Baseline	✗	✗	90.29	-
MIND _{base} w/o P2CL	✗	✓	90.36	0.07 ↑
MIND _{base} w/o MCA	✓	✗	92.15	1.86 ↑
MIND_{base} (Ours)	✓	✓	92.29	2.00 ↑

Table 5. Performance analysis of generating rationales using different large models on the ScienceQA dataset.

Large Models	Acc.	Large Models	Acc.
Baseline	90.29	DeepseekR1-Qwen8B [12]	91.49
Qwen3-235B-22A [65]	91.61	Deepseek-R1 [12]	90.73
DeepseekV3 [29]	90.87	Final Mix	92.29

Table 6. Performance analysis of different numbers of rationales on the ScienceQA dataset. “ $\times N$ ” denotes N -fold expansion.

Rationales	Acc.	Rationales	Acc.
Original (21K)	90.29	$\times 100$ (2.1M)	91.58 (1.29 ↑)
$\times 10$ (210K)	91.42 (1.13 ↑)	$\times 500$ (10.5M)	91.91 (1.62 ↑)
$\times 50$ (1.05M)	91.56 (1.27 ↑)	$\times 1000$ (21M)	92.29 (2.00 ↑)

Table 7. Performance analysis of visual feature extraction methods on the ScienceQA dataset. **VFE**: Visual feature extraction

VFE Models	Acc.	VFE Models	Acc.
SAM-Base [22]	90.80	SAM-Huge [22]	91.25
DINOv2-Large [42]	91.06	DINOv2-Giant [42]	91.51
CLIP-B16 [44]	91.51	CLIP-L14-336 [44]	91.98
BLIP-Large [25]	91.49	BLIP2-flan-t5-xxL [26]	92.29

Table 8. Performance comparison of MIND with different settings on the ScienceQA dataset. The left and right arrows indicate the injection operations at the input and supervision of P2CL-II, respectively. **Pos**: Positive rationales. **Neg**: Negative Rationales.

Schemes	Acc.	Schemes	Acc.
MIND w/o P2CL-I	91.63	MIND w/o P2CL-II	90.36
Pos → N/A	91.20	Pos → Pos	91.20
Neg → N/A	90.64	Neg → Pos	91.72
Pos → N/A or Neg → N/A	91.37	Pos → Pos or Neg → N/A	91.39
Pos → N/A or Neg → Pos	91.96	Pos → Pos or Neg → Pos	92.29

4.5. Discuss “Understand → Rethink → Correct”

From Tab. 8, first, removing the P2CL-I alone leads to a 0.66% (from 92.29% to 91.63%) performance drop, indicating that semantic consistency learning lays the foundation for model understanding. At the same time, removing the P2CL-II stage alone resulted in a significant performance decrease of 1.93% (from 92.29% to 90.36%), which validates the core role of active logic discrimination and correction. Second, when the model outputs only an answer, providing a positive rationale input is more effective than a negative one, because positive semantics help stabilize logical structure, whereas negative rationales can drift without correction signals. Interestingly, The latter still outperforms removing P2CL-II entirely. This indicates that negative ra-

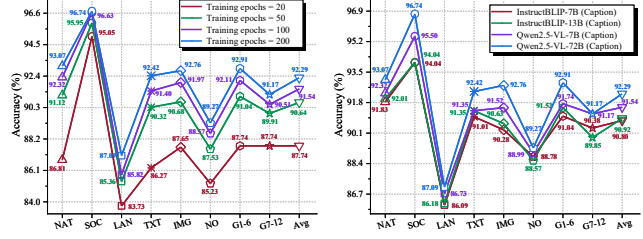


Figure 4. Performance analysis of Epochs and Caption generation methods on the ScienceQA dataset.

tionales provide adversarial cognitive stimulation, prompting the model to develop the ability to distinguish between correct and incorrect logic. Third, injecting a negative rationale input while supervising with a positive one yields notable gains. Specifically, compared to “*Neg* → *N/A*”, “*Neg* → *Pos*” directly improves 1.08% (from 90.64% to 91.72%); compared to “*Pos* → *N/A* or *Neg* → *N/A*”, “*Pos* → *N/A* or *Neg* → *Pos*” directly improves 0.59% (from 91.37 to 91.96). This demonstrates that the joint design of negative rationale input and positive rationale supervision enables explicit logic correction, allowing the model to transition from error identification to logic reconstruction. Finally, the model performs best when it mixes positive and negative rationales at the input while using positive rationale supervision. In summary, the P2CL strategy effectively realizes a progressive reasoning mechanism of “Understand → Rethink → Correct” through semantic understanding of P2CL-I and logic discrimination and correction of P2CL-II, enabling the model to have stronger logical stability and error correction capabilities, and achieving a paradigm evolution from passive imitation-based reasoning to active discriminative reasoning.

5. Conclusion

This paper introduces a MIND reasoning framework for MLLMs, aiming to endow the model with human-like cognitive pattern of “Understand → Rethink → Correct”, thereby achieving a paradigm evolution from passive imitation-based reasoning to active discriminative reasoning. Specifically, we propose a RAD paradigm, which provides a unified, scalable and high-quality data foundation. At the same time, a P2CL strategy is designed that enables multi-rationale positive learning and active logic discrimination and correction. In addition, a MCA optimization strategy is proposed to further enhance the model’s logical consistency and discriminative capability. Experimental results show that our MIND achieves SOTA performance on the ScienceQA, A-OKVQA, and M³CoT datasets, exhibiting stronger generalization and interpretability. We hope that this work can draw attention to the research on multi-rationale discrimination reasoning and promote MLLMs towards a new stage of intelligent reasoning.

References

[1] Josh Achiam, Steven Adler, Sandhini Agarwal, Lama Ahmad, Ilge Akkaya, Florencia Leoni Aleman, Diogo Almeida, Janko Altenschmidt, Sam Altman, Shyamal Anadkat, et al. Gpt-4 technical report. *arXiv preprint arXiv:2303.08774*, 2023. 6, 7

[2] Peter Anderson, Xiaodong He, Chris Buehler, Damien Teney, Mark Johnson, Stephen Gould, and Lei Zhang. Bottom-up and top-down attention for image captioning and visual question answering. In *CVPR*, pages 6077–6086, 2018. 6

[3] Shuai Bai, Keqin Chen, Xuejing Liu, Jialin Wang, Wenbin Ge, Sibo Song, Kai Dang, Peng Wang, Shijie Wang, Jun Tang, et al. Qwen2. 5-vl technical report. *arXiv preprint arXiv:2502.13923*, 2025. 5, 7

[4] Qiguang Chen, Libo Qin, Jin Zhang, Zhi Chen, Xiao Xu, and Wanxiang Che. m^3 cot: A novel benchmark for multi-domain multi-step multi-modal chain-of-thought. *arXiv preprint arXiv:2405.16473*, 2024. 1, 3, 5, 12

[5] Zhenfang Chen, Qinhong Zhou, Yikang Shen, Yining Hong, Hao Zhang, and Chuang Gan. See, think, confirm: Interactive prompting between vision and language models for knowledge-based visual reasoning. *arXiv preprint arXiv:2301.05226*, 2023. 2, 5, 6

[6] Zihui Cheng, Qiguang Chen, Jin Zhang, Hao Fei, Xiaocheng Feng, Wanxiang Che, Min Li, and Libo Qin. Comt: A novel benchmark for chain of multi-modal thought on large vision-language models. In *AAAI*, pages 23678–23686, 2025. 1

[7] Hyung Won Chung, Le Hou, Shayne Longpre, Barret Zoph, Yi Tay, William Fedus, Yunxuan Li, Xuezhi Wang, Mostafa Dehghani, Siddhartha Brahma, et al. Scaling instruction-finetuned language models. *Journal of Machine Learning Research*, 25(70):1–53, 2024. 5

[8] Wenliang Dai, Junnan Li, Dongxu Li, Anthony Tiong, Junqi Zhao, Weisheng Wang, Boyang Li, Pascale N Fung, and Steven Hoi. Instructblip: Towards general-purpose vision-language models with instruction tuning. *Advances in neural information processing systems*, 36:49250–49267, 2023. 7

[9] Yuhao Dong, Zuyan Liu, Hai-Long Sun, Jingkang Yang, Winston Hu, Yongming Rao, and Ziwei Liu. Insight-v: Exploring long-chain visual reasoning with multimodal large language models. In *CVPR*, pages 9062–9072, 2025. 1, 2

[10] Peng Gao, Zhengkai Jiang, Haoxuan You, Pan Lu, Steven CH Hoi, Xiaogang Wang, and Hongsheng Li. Dynamic fusion with intra-and inter-modality attention flow for visual question answering. In *CVPR*, pages 6639–6648, 2019. 6

[11] Timin Gao, Peixian Chen, Mengdan Zhang, Chaoyou Fu, Yunhang Shen, Yan Zhang, Shengchuan Zhang, Xiawu Zheng, Xing Sun, Liujuan Cao, et al. Cantor: Inspiring multimodal chain-of-thought of mllm. In *Proceedings of the ACM International Conference on Multimedia (ACM MM)*, pages 9096–9105, 2024. 2

[12] Daya Guo, Dejian Yang, Haowei Zhang, Junxiao Song, Ruoyu Zhang, Runxin Xu, Qihao Zhu, Shirong Ma, Peiyi Wang, Xiao Bi, et al. Deepseek-r1: Incentivizing reasoning capability in llms via reinforcement learning. *arXiv preprint arXiv:2501.12948*, 2025. 7, 8

[13] Liqi He, Zuchao Li, Xiantao Cai, and Ping Wang. Multi-modal latent space learning for chain-of-thought reasoning in language models. In *AAAI*, pages 18180–18187, 2024. 1, 2, 5, 6

[14] Yushi Hu, Weijia Shi, Xingyu Fu, Dan Roth, Mari Ostendorf, Luke Zettlemoyer, Noah A Smith, and Ranjay Krishna. Visual sketchpad: Sketching as a visual chain of thought for multimodal language models. *Advances in Neural Information Processing Systems*, 37:139348–139379, 2024. 2

[15] Xiaoshuang Huang, Lingdong Shen, Jia Liu, Fangxin Shang, Hongxiang Li, Haifeng Huang, and Yehui Yang. Towards a multimodal large language model with pixel-level insight for biomedicine. In *AAAI*, pages 3779–3787, 2025. 1

[16] Anubhooti Jain, Mayank Vatsa, and Richa Singh. Words over pixels? rethinking vision in multimodal large language models. In *Proceedings of the International Joint Conference on Artificial Intelligence (IJCAI)*, pages 10481–10489, 2024. 1

[17] Yu Jiang, Vivek Natarajan, Xinlei Chen, Marcus Rohrbach, Dhruv Batra, and Devi Parikh. Pythia v0. 1: the winning entry to the vqa challenge 2018. *arXiv preprint arXiv:1807.09956*, 2018. 6

[18] Amita Kamath, Christopher Clark, Tanmay Gupta, Eric Kolve, Derek Hoiem, and Aniruddha Kembhavi. Webly supervised concept expansion for general purpose vision models. In *ECCV*, pages 662–681. Springer, 2022. 6

[19] Daniel Khashabi, Sewon Min, Tushar Khot, Ashish Sabharwal, Oyvind Tafjord, Peter Clark, and Hannaneh Hajishirzi. Unifiedqa: Crossing format boundaries with a single qa system. *arXiv preprint arXiv:2005.00700*, 2020. 6

[20] Jin-Hwa Kim, Jaehyun Jun, and Byoung-Tak Zhang. Bi-linear attention networks. *Advances in neural information processing systems*, 31, 2018. 6

[21] Wonjae Kim, Bokyung Son, and Ildoo Kim. Vilt: Vision-and-language transformer without convolution or region supervision. In *Proceedings of the International Conference on Machine Learning (ICML)*, pages 5583–5594. PMLR, 2021. 6

[22] Alexander Kirillov, Eric Mintun, Nikhila Ravi, Hanzi Mao, Chloe Rolland, Laura Gustafson, Tete Xiao, Spencer Whitehead, Alexander C Berg, Wan-Yen Lo, et al. Segment anything. In *Proceedings of the IEEE/CVF International Conference on Computer Vision (ICCV)*, pages 4015–4026, 2023. 7, 8

[23] Jing Yu Koh, Daniel Fried, and Russ R Salakhutdinov. Generating images with multimodal language models. *Advances in Neural Information Processing Systems*, 36:21487–21506, 2023. 2

[24] Junlin Lee, Yequan Wang, Jing Li, and Min Zhang. Multi-modal reasoning with multimodal knowledge graph. *arXiv preprint arXiv:2406.02030*, 2024. 2

[25] Junnan Li, Dongxu Li, Caiming Xiong, and Steven Hoi. Blip: Bootstrapping language-image pre-training for unified vision-language understanding and generation. In *ICML*, pages 12888–12900. PMLR, 2022. 8

[26] Junnan Li, Dongxu Li, Silvio Savarese, and Steven Hoi. Blip-2: Bootstrapping language-image pre-training with

frozen image encoders and large language models. In *ICML*, pages 19730–19742. PMLR, 2023. 5, 7, 8

[27] Liunian Harold Li, Mark Yatskar, Da Yin, Cho-Jui Hsieh, and Kai-Wei Chang. What does bert with vision look at? In *Proceedings of the Association for Computational Linguistics (ACL)*, pages 5265–5275, 2020. 6

[28] Zejun Li, Ruiyu Luo, Jiwen Zhang, Minghui Qiu, Xuan-Jing Huang, and Zhongyu Wei. Vocot: Unleashing visually grounded multi-step reasoning in large multi-modal models. In *Proceedings of the Conference of the North American Chapter of the Association for Computational Linguistics: Human Language Technologies (NAACL-HLT)*, pages 3769–3798, 2025. 2

[29] Aixin Liu, Bei Feng, Bing Xue, Bingxuan Wang, Bochao Wu, Chengda Lu, Chenggang Zhao, Chengqi Deng, Chenyu Zhang, Chong Ruan, et al. Deepseek-v3 technical report. *arXiv preprint arXiv:2412.19437*, 2024. 7, 8

[30] Bingshuai Liu, Chenyang Lyu, Zijun Min, Zhanyu Wang, Jinsong Su, and Longyue Wang. Retrieval-augmented multi-modal chain-of-thoughts reasoning for large language models. *arXiv preprint arXiv:2312.01714*, 2023. 2

[31] Haotian Liu, Chunyuan Li, Yuheng Li, and Yong Jae Lee. Improved baselines with visual instruction tuning. In *CVPR*, pages 26296–26306, 2024. 5, 6, 7

[32] Jiasen Lu, Dhruv Batra, Devi Parikh, and Stefan Lee. Vilbert: Pretraining task-agnostic visiolinguistic representations for vision-and-language tasks. *Advances in neural information processing systems*, 32, 2019. 6

[33] Pan Lu, Liang Qiu, Jiaqi Chen, Tony Xia, Yizhou Zhao, Wei Zhang, Zhou Yu, Xiaodan Liang, and Song-Chun Zhu. Iconqa: A new benchmark for abstract diagram understanding and visual language reasoning. *arXiv preprint arXiv:2110.13214*, 2021. 6

[34] Pan Lu, Swaroop Mishra, Tanglin Xia, Liang Qiu, Kai-Wei Chang, Song-Chun Zhu, Oyvind Tafjord, Peter Clark, and Ashwin Kalyan. Learn to explain: Multimodal reasoning via thought chains for science question answering. *Advances in Neural Information Processing Systems*, 35:2507–2521, 2022. 3, 5, 6, 12

[35] Pan Lu, Baolin Peng, Hao Cheng, Michel Galley, Kai-Wei Chang, Ying Nian Wu, Song-Chun Zhu, and Jianfeng Gao. Chameleon: Plug-and-play compositional reasoning with large language models. *Advances in Neural Information Processing Systems*, 36:43447–43478, 2023. 6, 7

[36] Gen Luo, Yiyi Zhou, Tianhe Ren, Shengxin Chen, Xiaoshuai Sun, and Rongrong Ji. Cheap and quick: Efficient vision-language instruction tuning for large language models. *Advances in Neural Information Processing Systems*, 36:29615–29627, 2023. 6

[37] Xuwen Luo, Fan Ding, Yinsheng Song, Xiaofeng Zhang, and Junnyong Loo. Pkrd-cot: A unified chain-of-thought prompting for multi-modal large language models in autonomous driving. In *Proceedings of the International Conference on Neural Information Processing (ICONIP)*, pages 62–76. Springer, 2024. 2

[38] Kenneth Marino, Xinlei Chen, Devi Parikh, Abhinav Gupta, and Marcus Rohrbach. Krisp: Integrating implicit and symbolic knowledge for open-domain knowledge-based vqa. In *CVPR*, pages 14111–14121, 2021. 6

[39] Fanxu Meng, Haotong Yang, Yiding Wang, and Muhan Zhang. Chain of images for intuitively reasoning. *arXiv preprint arXiv:2311.09241*, 2023. 2

[40] Chancharik Mitra, Brandon Huang, Trevor Darrell, and Roei Herzig. Compositional chain-of-thought prompting for large multimodal models. In *CVPR*, pages 14420–14431, 2024. 2

[41] Ron Mokady, Amir Hertz, and Amit H Bermano. Clipcap: Clip prefix for image captioning. *arXiv preprint arXiv:2111.09734*, 2021. 6

[42] Maxime Oquab, Timothée Darcet, Théo Moutakanni, Huy Vo, Marc Szafraniec, Vasil Khalidov, Pierre Fernandez, Daniel Haziza, Francisco Massa, Alaaeldin El-Nouby, et al. Dinov2: Learning robust visual features without supervision. *arXiv preprint arXiv:2304.07193*, 2023. 7, 8

[43] Zhiliang Peng, Wenhui Wang, Li Dong, Yaru Hao, Shaohan Huang, Shuming Ma, and Furu Wei. Kosmos-2: Grounding multimodal large language models to the world. *arXiv preprint arXiv:2306.14824*, 2023. 7

[44] Alec Radford, Jong Wook Kim, Chris Hallacy, Aditya Ramesh, Gabriel Goh, Sandhini Agarwal, Girish Sastry, Amanda Askell, Pamela Mishkin, Jack Clark, et al. Learning transferable visual models from natural language supervision. In *ICML*, pages 8748–8763. PMLR, 2021. 7, 8

[45] Colin Raffel, Noam Shazeer, Adam Roberts, Katherine Lee, Sharan Narang, Michael Matena, Yanqi Zhou, Wei Li, and Peter J Liu. Exploring the limits of transfer learning with a unified text-to-text transformer. *Journal of machine learning research*, 21(140):1–67, 2020. 5

[46] Dustin Schwenk, Apoorv Khandelwal, Christopher Clark, Kenneth Marino, and Roozbeh Mottaghi. A-okvqa: A benchmark for visual question answering using world knowledge. In *ECCV*, pages 146–162. Springer, 2022. 3, 5, 12

[47] Yongliang Shen, Kaitao Song, Xu Tan, Dongsheng Li, Weiming Lu, and Yueteng Zhuang. Hugginggpt: Solving ai tasks with chatgpt and its friends in hugging face. *Advances in Neural Information Processing Systems*, 36:38154–38180, 2023. 6, 7

[48] Mukul Singh, José Cambronero, Sumit Gulwani, Vu Le, and Gust Verbruggen. Assessing gpt4-v on structured reasoning tasks. *arXiv preprint arXiv:2312.11524*, 2023. 2

[49] Cheng Tan, Jingxuan Wei, Zhangyang Gao, Linzhuang Sun, Siyuan Li, Ruifeng Guo, Bihui Yu, and Stan Z Li. Boosting the power of small multimodal reasoning models to match larger models with self-consistency training. In *ECCV*, pages 305–322. Springer, 2024. 1, 2, 5, 6, 7

[50] Cheng Tan, Jingxuan Wei, Linzhuang Sun, Zhangyang Gao, Siyuan Li, Bihui Yu, Ruifeng Guo, and Stan Z Li. Retrieval meets reasoning: Even high-school textbook knowledge benefits multimodal reasoning. *arXiv preprint arXiv:2405.20834*, 2024. 2, 6

[51] Hao Tan and Mohit Bansal. Lxmert: Learning cross-modality encoder representations from transformers. *arXiv preprint arXiv:1908.07490*, 2019. 6

[52] Gemini Team, Rohan Anil, Sebastian Borgeaud, Jean-Baptiste Alayrac, Jiahui Yu, Radu Soricut, Johan Schalkwyk,

Andrew M Dai, Anja Hauth, Katie Millican, et al. Gemini: a family of highly capable multimodal models. *arXiv preprint arXiv:2312.11805*, 2023. 6, 7

[53] Weijie Tu, Weijian Deng, Dylan Campbell, Yu Yao, Jiyang Zheng, Tom Gedeon, and Tongliang Liu. Ranked from within: Ranking large multimodal models without labels. In *ICML*, 2025. 1

[54] Jiayu Wang, Yifei Ming, Zhenmei Shi, Vibhav Vineet, Xin Wang, Sharon Li, and Neel Joshi. Is a picture worth a thousand words? delving into spatial reasoning for vision language models. *Advances in Neural Information Processing Systems*, 37:75392–75421, 2024. 1

[55] Lei Wang, Yi Hu, Jiabang He, Xing Xu, Ning Liu, Hui Liu, and Heng Tao Shen. T-sciq: Teaching multimodal chain-of-thought reasoning via large language model signals for science question answering. In *AAAI*, pages 19162–19170, 2024. 1, 2, 5, 6

[56] Weihan Wang, Qingsong Lv, Wenmeng Yu, Wenyi Hong, Ji Qi, Yan Wang, Junhui Ji, Zhuoyi Yang, Lei Zhao, Song Xi-Xuan, et al. Cogvlm: Visual expert for pretrained language models. *Advances in Neural Information Processing Systems*, 37:121475–121499, 2024. 7

[57] Xiaohan Wang, Yuhui Zhang, Orr Zohar, and Serena Yeung-Levy. Videoagent: Long-form video understanding with large language model as agent. In *ECCV*, pages 58–76. Springer, 2024. 2

[58] Yaoting Wang, Shengqiong Wu, Yuecheng Zhang, Shuicheng Yan, Ziwei Liu, Jiebo Luo, and Hao Fei. Multimodal chain-of-thought reasoning: A comprehensive survey. *arXiv preprint arXiv:2503.12605*, 2025. 1, 2

[59] Jason Wei, Xuezhi Wang, Dale Schuurmans, Maarten Bosma, Fei Xia, Ed Chi, Quoc V Le, Denny Zhou, et al. Chain-of-thought prompting elicits reasoning in large language models. *Advances in neural information processing systems*, 35:24824–24837, 2022. 6

[60] Chenfei Wu, Shengming Yin, Weizhen Qi, Xiaodong Wang, Zecheng Tang, and Nan Duan. Visual chatgpt: Talking, drawing and editing with visual foundation models. *arXiv preprint arXiv:2303.04671*, 2023. 7

[61] Jiannan Wu, Muyan Zhong, Sen Xing, Zeqiang Lai, Zhaoyang Liu, Zhe Chen, Wenhui Wang, Xizhou Zhu, Lewei Lu, Tong Lu, et al. Visionllm v2: An end-to-end generalist multimodal large language model for hundreds of vision-language tasks. *Advances in Neural Information Processing Systems*, 37:69925–69975, 2024. 1

[62] Wenshan Wu, Shaoguang Mao, Yadong Zhang, Yan Xia, Li Dong, Lei Cui, and Furu Wei. Mind’s eye of llms: visualization-of-thought elicits spatial reasoning in large language models. *Advances in Neural Information Processing Systems*, 37:90277–90317, 2024. 2

[63] Yifan Wu, Pengchuan Zhang, Wenhan Xiong, Barlas Ooguz, James C Gee, and Yixin Nie. The role of chain-of-thought in complex vision-language reasoning task. *arXiv preprint arXiv:2311.09193*, 2023. 2

[64] Jixuan Wu, Yizhou Wang, Shixiang Tang, Wenhao Wu, Tong He, Wanli Ouyang, Philip Torr, and Jian Wu. Detoolchain: A new prompting paradigm to unleash detection ability of mllm. In *ECCV*, pages 164–182. Springer, 2024. 2

[65] An Yang, Anfeng Li, Baosong Yang, Beichen Zhang, Binyuan Hui, Bo Zheng, Bowen Yu, Chang Gao, Chengan Huang, Chenxu Lv, et al. Qwen3 technical report. *arXiv preprint arXiv:2505.09388*, 2025. 7, 8

[66] Jihan Yang, Shusheng Yang, Anjali W Gupta, Rilyn Han, Li Fei-Fei, and Saining Xie. Thinking in space: How multimodal large language models see, remember, and recall spaces. In *CVPR*, pages 10632–10643, 2025. 1

[67] Shuo Yang, Caren Han, Siwen Luo, and Eduard Hovy. Magic-vqa: Multimodal and grounded inference with commonsense knowledge for visual question answering. In *Findings of the Association for Computational Linguistics (Findings of ACL)*, pages 16967–16986, 2025. 1

[68] Zhengyuan Yang, Zhe Gan, Jianfeng Wang, Xiaowei Hu, Yuanmao Lu, Zicheng Liu, and Lijuan Wang. An empirical study of gpt-3 for few-shot knowledge-based vqa. In *AAAI*, pages 3081–3089, 2022. 6

[69] Nicolas Yax, Hernán Anlló, and Stefano Palminteri. Studying and improving reasoning in humans and machines. *Communications Psychology*, 2(1):51, 2024. 1

[70] Haoxuan You, Rui Sun, Zhecan Wang, Long Chen, Gengyu Wang, Hammad Ayyubi, Kai-Wei Chang, and Shih-Fu Chang. Idealgpt: Iteratively decomposing vision and language reasoning via large language models. In *Findings of the Association for Computational Linguistics: EMNLP (Findings of EMNLP)*, pages 11289–11303, 2023. 7

[71] Zhou Yu, Jun Yu, Yuhao Cui, Dacheng Tao, and Qi Tian. Deep modular co-attention networks for visual question answering. In *CVPR*, pages 6281–6290, 2019. 5, 6

[72] Daoan Zhang, Junming Yang, Hanjia Lyu, Zijian Jin, Yuan Yao, Mingkai Chen, and Jiebo Luo. Cocot: Contrastive chain-of-thought prompting for large multimodal models with multiple image inputs. *arXiv preprint arXiv:2401.02582*, 2024. 2

[73] Renrui Zhang, Jiaming Han, Chris Liu, Peng Gao, Ao-jun Zhou, Xiangfei Hu, Shilin Yan, Pan Lu, Hongsheng Li, and Yu Qiao. Llama-adapter: Efficient fine-tuning of language models with zero-init attention. *arXiv preprint arXiv:2303.16199*, 2023. 6, 7

[74] Zhuosheng Zhang, Aston Zhang, Mu Li, Hai Zhao, George Karypis, and Alex Smola. Multimodal chain-of-thought reasoning in language models. *Transactions on Machine Learning Research*, 2024, 2024. 1, 2, 5, 6, 7, 12

[75] Qi Zhao, Shijie Wang, Ce Zhang, Changcheng Fu, Minh Quan Do, Nakul Agarwal, Kwonjoon Lee, and Chen Sun. Antgpt: Can large language models help long-term action anticipation from videos? *arXiv preprint arXiv:2307.16368*, 2023. 2

[76] Ge Zheng, Bin Yang, Jiajin Tang, Hong-Yu Zhou, and Sibei Yang. Ddcot: Duty-distinct chain-of-thought prompting for multimodal reasoning in language models. *Advances in Neural Information Processing Systems*, 36:5168–5191, 2023. 1, 2, 6

[77] Shanshan Zhong, Zhongzhan Huang, Shanghua Gao, Wushao Wen, Liang Lin, Marinka Zitnik, and Pan Zhou. Let’s think outside the box: Exploring leap-of-thought in large language models with creative humor generation. In *CVPR*, pages 13246–13257, 2024. 2

MIND: Multi-rationale INtegrated Discriminative Reasoning Framework for Multi-modal Large Models

Supplementary Material

In this Supplementary Material, we offer extra details and additional results to complement the main paper. In Sec. A, we provide more ablation experiments to fully explore the performance of the MIND reasoning framework. In Sec. B, we provide a detailed qualitative analysis on ScienceQA [34], A-OKVQA [46], and M³CoT [4] datasets.

A. More Ablation Experiments

In this section, we have added more break-down ablation experiments and conducted a detailed investigation of the MCA optimization strategy. Details are as follows:

1) More Break-Down Ablation. To more comprehensively analyze the independent contributions and synergistic gains of each core component, we conduct systematic ablation studies on the P2CL strategy and MCA optimization strategies across ScienceQA, A-OKVQA, and M³CoT datasets. The experimental results are shown in Tab. S1. First, compared to the “Baseline”, using only the MCA optimization strategy alone results in an accuracy improvement of 0.07% (from 90.29% to 90.36%) - 3.02% (from 52.67% to 55.69%), indicating that the MCA optimization strategy can enhancing reasoning consistency and improving the model’s discrimination sensitivity. Second, compared to the “Baseline”, using only the P2CL strategy alone results in an accuracy improvement of 1.86% (from 90.29% to 92.15%) - 4.28% (from 65.85% to 70.13%), indicating that multi-rationale positive learning and active logic discrimination and correction can effectively strengthen reasoning robustness. Finally, the MIND reasoning framework, combining the MCA and P2CL strategies, achieves the best results on each dataset. Specifically, compared to the “Baseline”, jointly applying MCA and P2CL strategies improves accuracy by 2.00% (from 90.29% to 92.29%) - 4.72% (from 65.85% to 70.57%). This illustrates the complementarity between the P2CL and MCA strategies. The P2CL strategy constructs reliable logic and enables error-correctable reasoning, whereas MCA optimization strategy sharpens semantic boundaries and strengthens contrastive discrimination. Their collaboration jointly optimizes semantic coherence and logical discrimination, thereby significantly enhancing the model’s reasoning capability.

2) Exploration of Hyperparameters in the MCA optimization Strategy. We conduct a systematic analysis under various parameter settings. From Fig. S1, the experimental results with different values of m and α demonstrate that the MCA optimization strategy has remarkable stability. In particular, when $m \in [0.1 - 0.4]$ and $\alpha \in [0.5 - 5.0]$,

Table S1. Break-Down ablation experiments on ScienceQA, A-OKVQA, and M³CoT datasets. “*Imp.*”: Improvement.

Schemes	P2CL	MCA	ScienceQA		A-OKVQA		M ³ CoT	
			Acc.	Imp.	Acc.	Imp.	Acc.	Imp.
Baseline	✗	✗	90.29	-	65.85	-	52.67	-
MIND _{base} w/o P2CL	✗	✓	90.36	0.07 ↑	68.03	2.18 ↑	55.69	3.02 ↑
MIND _{base} w/o MCA	✓	✗	92.15	1.86 ↑	70.13	4.28 ↑	56.34	3.67 ↑
MIND_{base} (Ours)	✓	✓	92.29	2.00 ↑	70.57	4.72 ↑	57.38	4.71 ↑

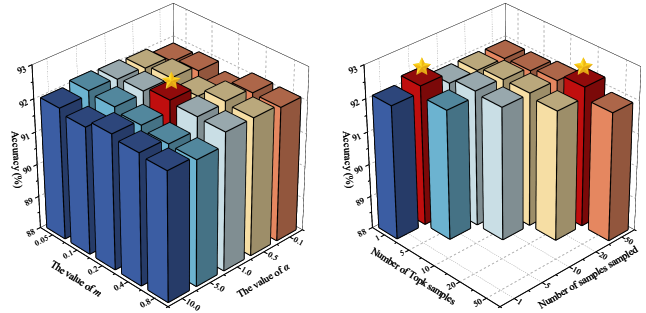


Figure S1. Exploring the hyperparameters of the MCA optimization strategy on the ScienceQA dataset. **Left:** m and α . **Right:** Sampled rationales and Top-k. Red bars denote the optimal.

the model performance remains stable and varies smoothly. The optimal performance is achieved when $m = 0.2$ and $\alpha = 1$. At the same time, from the system experiments of the sampling number and Top-k setting in Fig. S1, compared to the scheme that uses all samples in the outermost row, selecting the Top-k hard rationales under the same sampling scale can achieve higher performance. Specifically, the model achieves its best results when the (*sampled rationales*, *Top-k*) settings are (5, 1) and (50, 20), respectively. These findings indicate that maintaining rationale diversity while moderately focusing on hard rationales can effectively enhance the discriminative capability and semantic boundary modeling. Notably, MCA used the same hyperparameter settings in all other experiments.

B. Qualitative Analysis

In this section, we have provided a detailed qualitative analysis. Specifically, on the one hand, we qualitatively compare Multimodal-CoT [74] and MIND. On the other hand, we conduct a qualitative analysis of MIND’s Error-Correction capability. Details are as follows:

1) Comparison Between Multimodal-CoT and MIND.

To more intuitively demonstrate the superior interpretability and logical consistency of MIND in multimodal reason-

Question: Will these magnets attract or repel each other?

Options:

ScienceQA #843

A. attract

B. repel



Gold Rationale: Will these magnets attract or repel? To find out, look at which poles are closest to each other. The north pole of one magnet is closest to the north pole of the other magnet. Poles that are the same repel. So, these magnets will repel each other.

True Answer: The answer is (B).

Multimodal-CoT

MIND

Rationale: Will these magnets attract or repel? To find out, look at which poles are closest to each other. The south pole of one magnet is closest to the south pole of the other magnet. Poles that are different attract. So, these magnets will attract each other.

Answer: The answer is (A).

Rationale: To decide if the magnets attract or repel, check the poles closest to each other. The north pole of one magnet is near the north pole of the other. Like poles repel, so these magnets will repel.

Answer: The answer is (B). BECAUSE: The input Rationale is correct! To decide if the magnets attract or repel, check the poles closest to each other. The north pole of one magnet is near the north pole of the other. Like poles repel, so these magnets will repel.

Figure S2. Reasoning case comparison between $\text{MIND}_{\text{base}}$ and $\text{Multimodal-CoT}_{\text{base}}$ on selected samples from the ScienceQA dataset. Red denotes incorrect reasoning, green denotes correct reasoning, and “#” denotes the Question ID.

Question: They are likely having pizza at what kind of event?

Options:

A. family

B. gaming

C. academic

D. social

A-OKVQA #17111



Gold Rationale: The chairs and the relative ages of the people in the image is consistent with answer a. The people are mostly about the same age. they are sitting in desks. The men look like students.

True Answer: The answer is (C).

Multimodal-CoT

MIND

Rationale: The people are all dressed up and eating pizza. they are probably having a social pizza party. The people are dressed up and eating pizza. They are all dressed up and eating pizza.

Answer: The answer is (D).

Rationale: The group is eating pizza in an office setting. The pizza is a common sight at social events, but the context suggests a more casual, family-oriented gathering.

Answer: The answer is (C). BECAUSE: The input Rationale is incorrect! The correct one is as follows: The group is eating pizza in an office. Pizza is a staple at academic gatherings. They are in an office.

Figure S3. Reasoning case comparison between $\text{MIND}_{\text{base}}$ and $\text{Multimodal-CoT}_{\text{base}}$ on selected samples from the A-OKVQA dataset. Red denotes incorrect reasoning, green denotes correct reasoning, and “#” denotes the Question ID.

ing, we select one samples from each of the ScienceQA, A-OKVQA, and M^3CoT datasets for qualitative comparison with Multimodal-CoT. The visualization results are shown in Figs. S2 to S4. We observe that prior Multimodal-CoT often exhibit issues such as logical confusion and conclusion drift in scenes with visual ambiguity or semantic interference. In contrast, MIND learns a multi-rationale se-

mantic distribution during training, enabling it to adaptively focus on key semantic cues under complex inputs and produce reasoning results with stronger causal coherence. At the same time, our MIND uses active logic discrimination and correction in the Phase II (P2CL-II). When the input contains logical errors or misleading rationale, Multimodal-CoT tends to follow the flawed semantic direction and pro-

Question: Do you know the depth of the point farthest west?

Options:

A. 4.7 km B. 6.8 km C. 2.4 km D. 5.3 km

M³CoT #11139

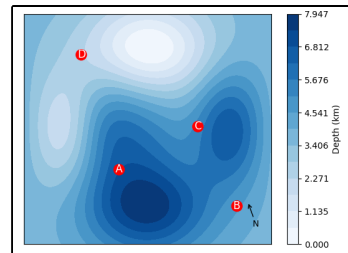
Gold Rationale:

Step 1: To start, pinpoint the directional marker on the map. The directional marker indicates the cardinal directions (North) and shows the orientation of the map.
 Step 2: Identify the westernmost point. The western extremity is represented by A.
 Step 3: Once you've located the westernmost point, seek out the contour lines that intersect with it or pass nearby. Map contour lines connect points with matching depths, demonstrating variations in height.
 Step 4: Ascertain the Depth.

- Identify the contour line that intersects or is nearest to the westernmost point.
- Read the corresponding color, and compare it with the color in the legend.
- We can roughly gauge that the depth stands at approximately 6.8 kilometers.

Step 5: Therefore, choice "(B) 6.8 km" is the answer.

True Answer: The answer is (B).



Multimodal-CoT

MIND

Rationale:

Step 1: First, locate the directional marker on the map. This marker signifies the cardinal directions (North) and indicates the map's orientation.

Step 2: Find the point farthest to the west. We can find that C the westernmost point.

Step 3: Once you've located the westernmost point, seek out the contour lines that intersect with it or pass nearby. Contour lines are lines on the map that connect points of equal depth. They represent changes in depth.

Step 4: Establishing the Depth.

- Locate the contour line that intersects or is nearest to the westernmost point.
- Analyze the associated color and match it with the legend.
- We can make an approximate estimate that the depth is around 6.8 kilometers.

Step 5: Hence, choice "(B) 6.8 km" is the answer.

Answer: The answer is (D).

Rationale:

Step 1: Start by locating the directional marker on the map. This marker shows the cardinal directions (North) and sets the map's orientation.

Step 2: Determine the westernmost point. Point A is the furthest west.

Step 3: After identifying the westernmost point, examine the contour lines that pass through or near it. These lines connect points of equal depth and show depth variations.

Step 4: Estimating the Depth.

- Find the contour line closest to or intersecting the westernmost point.
- Compare the color to the legend.
- The depth is roughly 6.8 km.

Step 5: Hence, the correct choice is "(B) 6.8 km."

Answer: The answer is (B). BECAUSE: The input Rationale is correct!

Step 1: Start by locating the directional marker on the map. This marker shows the cardinal directions (North) and sets the map's orientation.

Step 2: Determine the westernmost point. Point A is the furthest west.

Step 3: After identifying the westernmost point, examine the contour lines that pass through or near it. These lines connect points of equal depth and show depth variations.

Step 4: Estimating the Depth.

- Find the contour line closest to or intersecting the westernmost point.
- Compare the color to the legend.
- The depth is roughly 6.8 km.

Step 5: Hence, the correct choice is "(B) 6.8 km."

Figure S4. Reasoning case comparison between MIND_{base} and Multimodal-CoT_{base} on selected samples from the M³CoT dataset. Red denotes incorrect reasoning, green denotes correct reasoning, and “#” denotes the Question ID.

duce unreasonable conclusions. In comparison, MIND can actively detect reasoning deviations and reconstruct correct logic aligned with factual and visual semantics.

2) **MIND's Error-Correction Capability.** To more intuitively and comprehensively demonstrate how MIND can reflect on and correct flawed logic in the rationales gener-

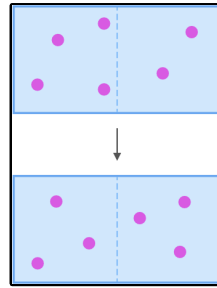
ated during Phase I (P2CL-I), we conduct qualitative analyses on some samples from each of the ScienceQA, A-OKVQA, and M³CoT datasets. The visualization results are shown in Figs. S5 to S7. In the cases presented, the *Rationale* generated in Phase I contains varying degrees of misleading logic, such as incorrect factual associations and

Question: Complete the text to describe the diagram. Solute particles moved in both directions across the permeable membrane. But more solute particles moved across the membrane (). When there was an equal concentration on both sides, the particles reached equilibrium.

Options:

A. to the left than to the right B. to the right than to the left

ScienceQA #13736



Gold Rationale: Look at the diagram again. It shows you how the solution changed during the process of diffusion. Before the solute particles reached equilibrium, there were 4 solute particles on the left side of the membrane and 2 solute particles on the right side of the membrane. When the solute particles reached equilibrium, there were 3 solute particles on each side of the membrane. There was 1 more solute particle on the right side of the membrane than before. So, for the solute particles to reach equilibrium, more solute particles must have moved across the membrane to the right than to the left.

True Answer: The answer is (B).

Phase I: Rationale generation

Phase II: Answer generation

Rationale: The diagram demonstrates diffusion. Initially, the left side had 4 particles, and the right side had 2. At equilibrium, both sides had 4 particles. The right side's gain of 1 particle indicates more movement to the right than to the left.

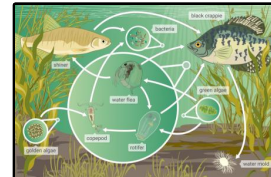
Answer: The answer is (B). BECAUSE: The input Rationale is incorrect! The correct one is as follows: The diagram illustrates diffusion. Initially, 4 particles were on the left and 2 on the right. At equilibrium, both sides had 3 particles, indicating more particles moved to the right.

Question: Which of the following organisms is the decomposer in this food web?

Options:

A. green algae B. water mold C. golden algae

ScienceQA #1392



Gold Rationale: Decomposers help break down dead organisms into simpler matter, such as nutrients. These nutrients can then help plants and other organisms grow. In a food web, there is an arrow pointing from another organism to a decomposer. There are no arrows pointing from a decomposer to another organism. The water mold does not have arrows pointing from it to other organisms. So, the water mold is a decomposer. The bacteria do not have arrows pointing from them to other organisms. So, the bacteria are decomposers. The green algae has arrows pointing from it. So, the green algae is not a decomposer. The golden algae has an arrow pointing from it. So, the golden algae is not a decomposer.

True Answer: The answer is (B).

Phase I: Rationale generation

Phase II: Answer generation

Rationale: Decomposers break down dead organisms into simpler nutrients, supporting plants and other organisms. In food webs, arrows point to decomposers, not from them. Green algae has arrows pointing to it, so it's not a decomposer. Water mold has arrows pointing to it, so it's not a decomposer. Golden algae has arrows pointing to it, so it's not a decomposer.

Answer: The answer is (B). BECAUSE: The input Rationale is incorrect! The correct one is as follows: Decomposers break down dead organisms into simpler nutrients, supporting plants and other organisms. In food webs, arrows point to decomposers, but not from them. Green algae has outgoing arrows, so it's not a decomposer. Water mold has no outgoing arrows, so it's a decomposer. Golden algae has outgoing arrows, so it's not a decomposer. Water mold has no outgoing arrows, so it's a decomposer.

Figure S5. Some error correction cases of MIND_{base} on the ScienceQA dataset. Red denotes incorrect reasoning, green denotes correct reasoning, and “#” denotes the Question ID. The proposed MIND reasoning framework demonstrates excellent error correction capabilities.

logical leaps. For these *Rationales* with reasoning biases, our MIND exhibits strong reflective and corrective abilities in Phase II (P2CL-II). The model can detect key semantic conflicts that are inconsistent with the image, question, or ground-truth answer, and then generate revised Rationales that are both visually grounded and logically coherent.

From Figs. S5 to S7, in all scenarios including scientific reasoning (ScienceQA), open-domain common sense reasoning (A-OKVQA), and cross-domain complex reasoning (M³CoT), our MIND is able to recover to the correct log-

Question: The man is looking in what direction?

Options:

A. up

B. behind

C. sideways

D. down

A-OKVQA #17304



Gold Rationale: There are kites flying in the sky above the man. he is looking at them. The man is holding a kite and is looking in the direction of the kite that is in the air. He's looking at the flying kites.

True Answer: The answer is (A).

Phase I: Rationale generation

Phase II: Answer generation

Rationale: The man is looking backward. He is looking at the kite from behind. His gaze is directed at the kite, not the ground.

Answer: The answer is (A). BECAUSE: The input Rationale is incorrect! The correct one is as follows: The man is looking up. He is observing the kite from above. His gaze is directed at the kite, not the ground.

Question: What kind of cake is in the bottom row?

Options:

A. red velvet

B. cherry

C. lemon meringue

D. apple

A-OKVQA #17623



Gold Rationale: This kind of cake is known for its texture and color, giving it its name. The cake is red. The coloring of this cake will give it away upon seeing it. it is usually topped with a cream cheese icing.

True Answer: The answer is (A).

Phase I: Rationale generation

Phase II: Answer generation

Rationale: The cake in the bottom row is a cherry. Its spherical shape and reddish color are clear indicators.

Answer: The answer is (A). BECAUSE: The input Rationale is incorrect! The correct one is as follows: The bottom row's cake is red velvet. Its petite size and reddish hue are unmistakable.

Question: What type of parking is available?

Options:

A. truck

B. airplane

C. bicycle

D. rv

A-OKVQA #17115



Gold Rationale: There are bicycles clearly visible and parked on a rail specifically designed for parking. the other vehicles aren't visible and would not fit in this image. The bicycles are parked here. There are bikes out.

True Answer: The answer is (C).

Phase I: Rationale generation

Phase II: Answer generation

Rationale: The street has parking for cars. The parked cars are rvs. There are vehicles parked outside the building, and the rv is visible.

Answer: The answer is (C). BECAUSE: The input Rationale is incorrect! The correct one is as follows: The street is a parking zone for bicycles. The parked vehicles are bicycles. There are vehicles outside the building, and the bicycle is visible.

Figure S6. Some error correction cases of MIND_{base} on the A-OKVQA dataset. Red denotes incorrect reasoning, green denotes correct reasoning, and “#” denotes the Question ID. The proposed MIND reasoning framework demonstrates excellent error correction capabilities.

ical trajectory, further validating its human-like reasoning pattern of “Understand → Rethink → Correct”. MIND not only produces high-quality rationales but also possesses ac-

tive logic discrimination and correction, which is one of the key factors enabling its significant performance improvements over existing multimodal CoT methods.

Question: What does the arrangement of the geometric shapes in the image represent?

Options:

- A. A car
- B. A boat
- C. A bird
- D. A house

M³CoT #10742



Gold Rationale: The image consists of five different colored geometrical shapes arranged to represent the shape of a bird. The lemon-colored shape represents the neck, while the amber shape represents the body, and the orange shape represents the head. The mint shape forms the wing while the black shape is the tail feather. Therefore, the correct answer is C) A bird.

True Answer: The answer is (C).

Phase I: Rationale generation

Phase II: Answer generation

Rationale: The image features a Tangram puzzle arranged to resemble a bird. The body is represented by the ivory piece, the wings by the black piece, the legs by the pewter piece, and the tail by the ivory piece. Consequently, the correct answer is option b) A boat.

Answer: The answer is (C). BECAUSE: The input Rationale is incorrect! The correct one is as follows: The image displays a Tangram puzzle arranged to resemble a bird. The ivory piece is the body, the black piece the wings, the pewter piece the legs, and the ivory piece the tail. Consequently, the correct answer is option c) A bird.

Question: What kind of place is this most likely to be?

Options:

- A. A motorcycle gang meetup spot
- B. A shopping mall
- C. A park
- D. A restaurant

M³CoT #9153



Gold Rationale: The motorcycles lined up on the street together suggest that this place is a gathering spot for a motorcycle gang. There are many people here. The booths lined up in the background suggest that there are food stalls. Many green trees in the background suggest that this place could be a park. Based on the inferences, it is most likely that this is a park (C) rather than a motorcycle gang meetup spot, a shopping mall, or a restaurant.

True Answer: The answer is (C).

Phase I: Rationale generation

Phase II: Answer generation

Rationale: The motorcycles parked in a row on the pavement, indicating a motorcycle-centric setting, and the green stalls positioned nearby suggest a food-serving area. The gathered crowd indicates a social gathering, typical of a motorcycle gang meetup spot. The greenery indicates a green space, which is often used for public events. Therefore, the correct answer is A) A motorcycle gang meetup spot.

Answer: The answer is (C). BECAUSE: The input Rationale is incorrect! The correct one is as follows: The presence of motorcycles parked in a row on the pavement indicates a public area, and the green stalls positioned nearby suggest a food-serving area. The crowd gathered indicates a social gathering, typical of a motorcycle gang meetup spot. The greenery indicates a green space, often used for public events. Therefore, the correct answer is C) A park.

Figure S7. Some error correction cases of MIND_{base} on the M³CoT dataset. Red denotes incorrect reasoning, green denotes correct reasoning, and “#” denotes the Question ID. The proposed MIND reasoning framework demonstrates excellent error correction capabilities.